西安交通大學
XI'AN JIAOTONG UNIVERSITY

西安交通大學醫學院 XI'AN JIAOTONG UNIVERSITY COLLEGE OF MEDICINE
第二附属医院 (西北医院)

High-quality coronary artery segmentation via fuzzy logic modeling coupled with dynamic graph convolutional network

汇报人：董彩霞
2023年8月2日

研究背景

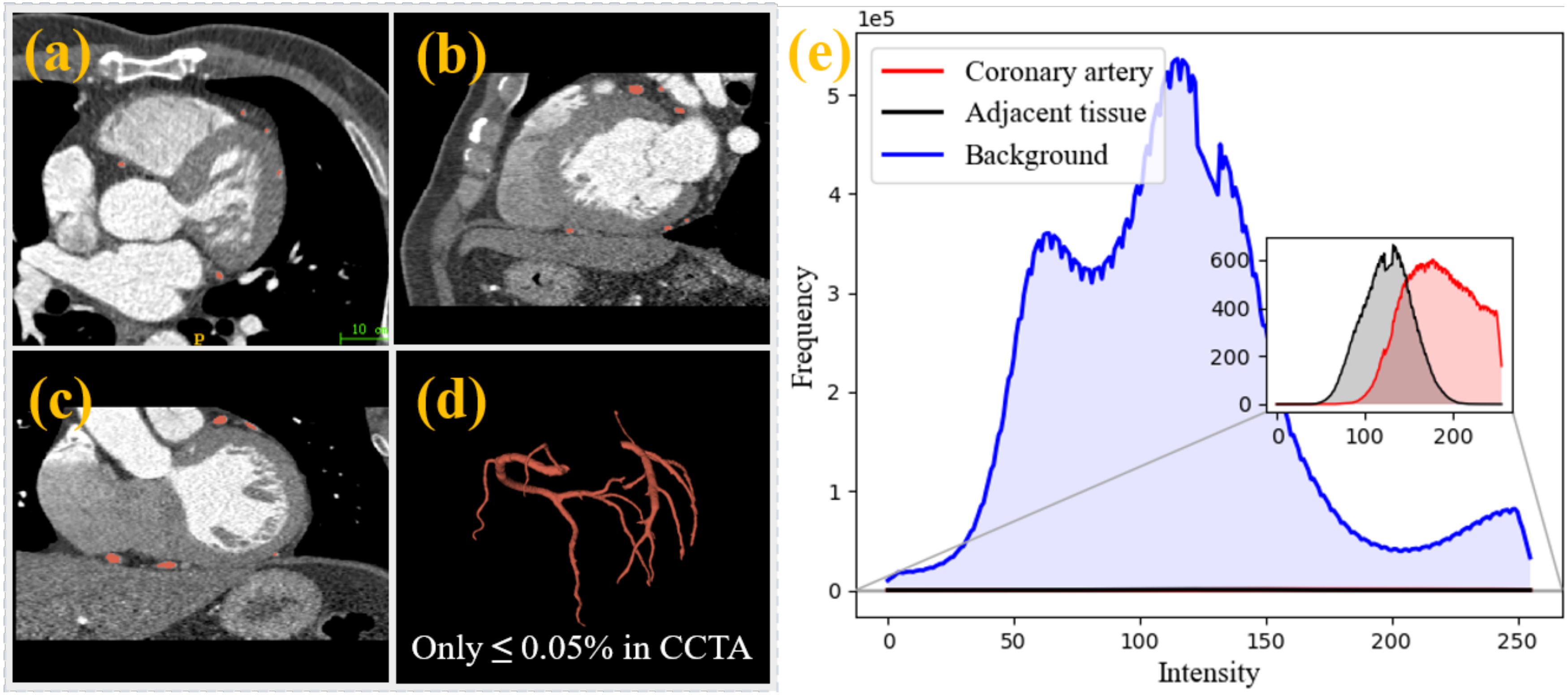

- Vessels are **thin structures** with lumen diameters ranging from 1 mm to 5 mm ((a)-(c)), leading to numerous **hard-to-segment regions and discontinuous segmentation**.
- The images have **a small volume ratio** (less than 0.05%, see (d)), which causes a severe imbalance between vessel and non-vessel pixels.
- The extremely **low contrast** in some vessel locations makes blood vessel boundaries ambiguous (1(e)).

方法：Framework

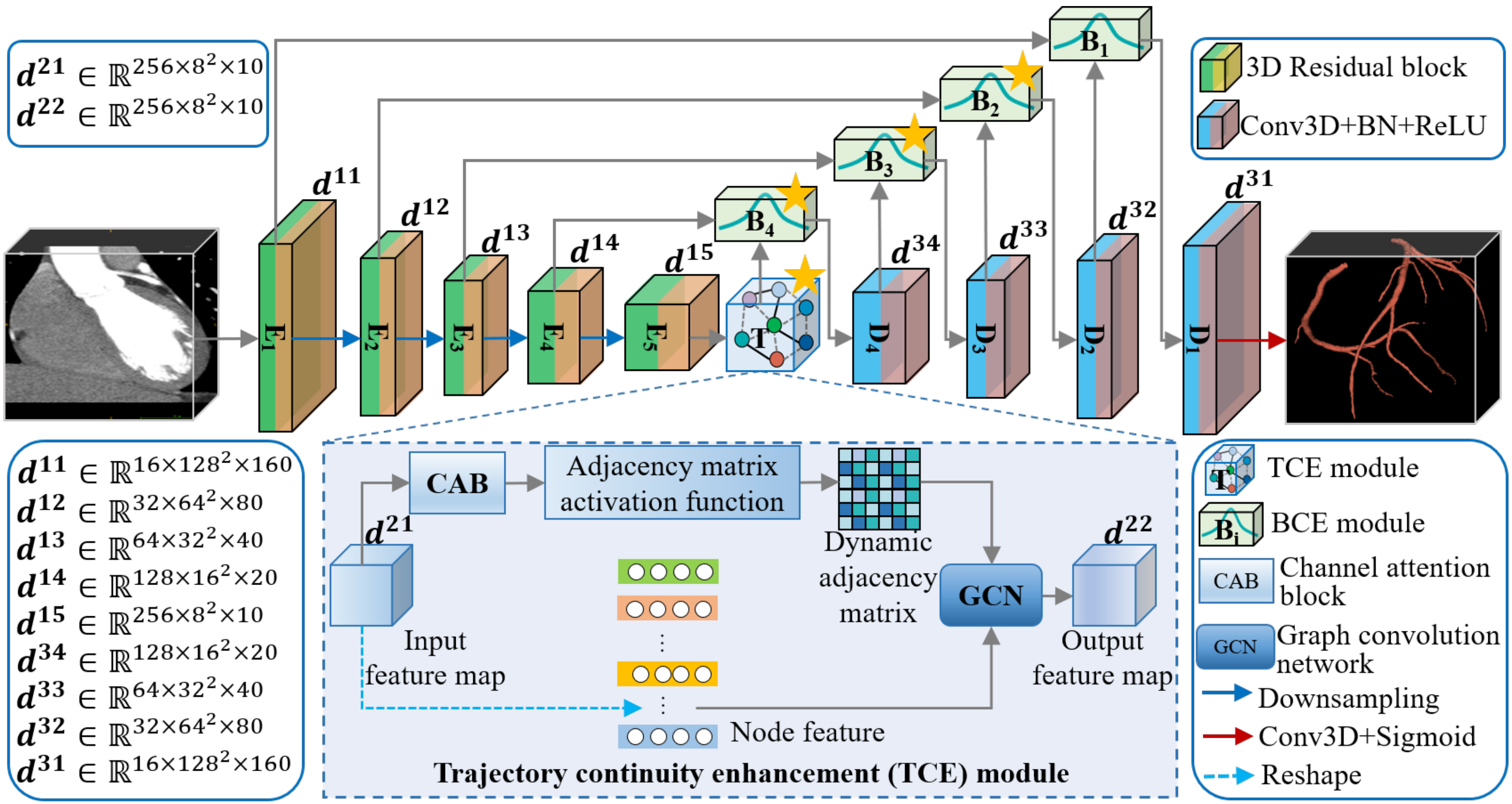

We propose a novel 3D deep network for high-quality CA segmentation that synergistically and comprehensively explores CA feature enhancement from the perspectives of **boundary completeness and trajectory continuity**, achieving a synergistic effect through the carefully orchestrated functioning of **fuzzy logic modeling coupled with a dynamic graph convolutional network**.

方法：Boundary Completeness Enhancement Module

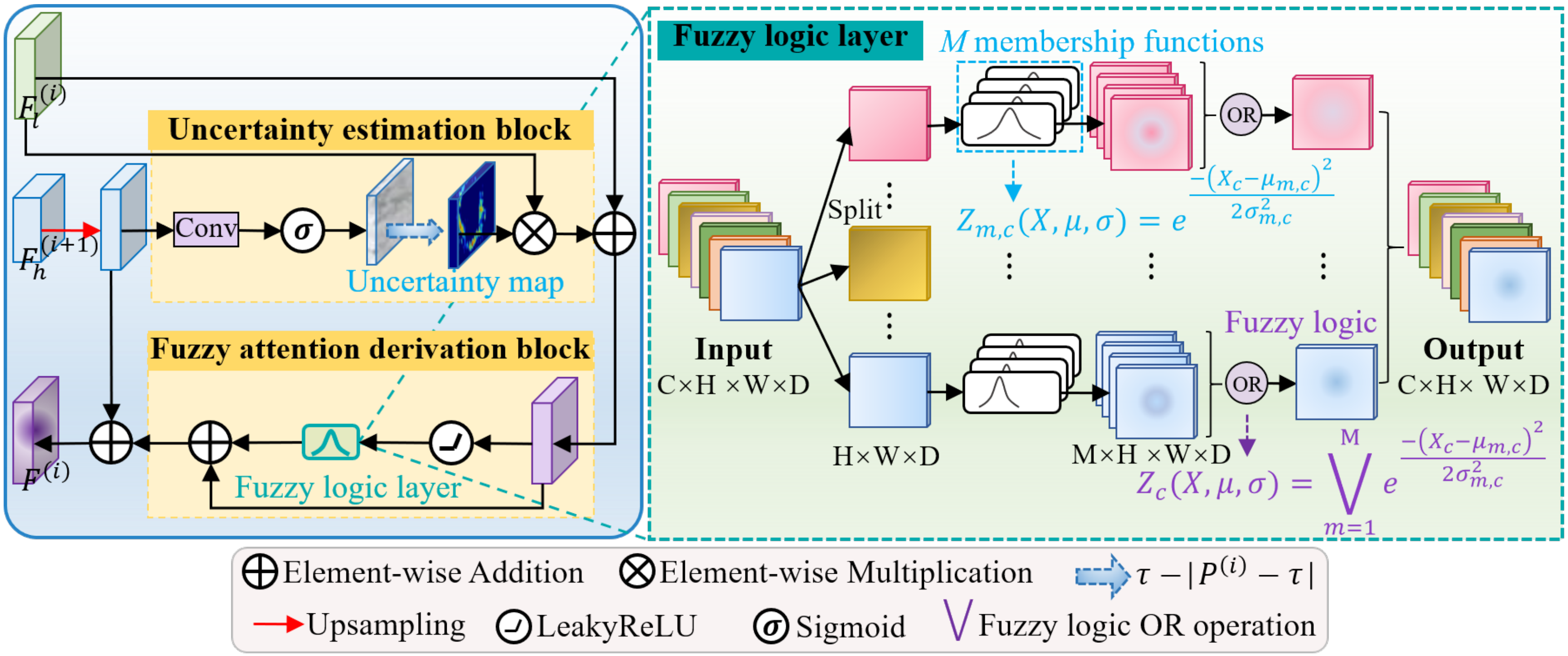

We propose a BCE module that integrates fuzzy logic with the attention mechanism to help the segmentation network focus on the relevant region while **reducing uncertainty** and variations in feature representations to improve **boundary quality**. It consists of two blocks: the **uncertainty estimation block** and the **fuzzy attention derivation block.**

方法：Boundary Completeness Enhancement Module

Algorithm 1 Boundary Completeness Enhancement Module

Input: The low-level features $F_l^{(i)}$ from encoder and high-level features $F_h^{(i+1)}$ from decoder.
Output: The enhanced feature representation $F^{(i)}$.

```
Randomly initialize parameters μ ∈ R^{m×C} and δ ∈ R^{m×C} of membership functions Z(X, μ, σ).
Compute the probability map P^{(i)} from the upper layer F_h^{(i+1)} of the decoder stream based on Eq.2.
for j in H × W × D do
    Compute the uncertainty estimation map Unc_j^{(i)} based on Eq.1.
end for
Compute the output F_{Unc}^{(i)} based on Eq.3.
Compute the input X ∈ R^{C×H×W×D} of the fuzzy logic layer, X = LeakyReLU(F_{Unc}^{(i)}).
for c in C do
    Compute the fuzzy membership degrees Z_c(X, μ, δ) based on Eq.4.
    Compute degrees Z_c(X, μ, δ) of c-th channel by adopting aggregation operator 'OR' to Z_c based on Eq.5.
end for
Compute the final result F^{(i)} of BCE based on Eq.6.
```

$$F_{Unc}^{(i)} = \left(Unc^{(i)} \otimes F_l^{(i)}\right) \oplus F_l^{(i)}$$

Uncertainty map: We believe that the closer the **predicted value is to the threshold τ**, the more **uncertain the prediction** of the corresponding position is.

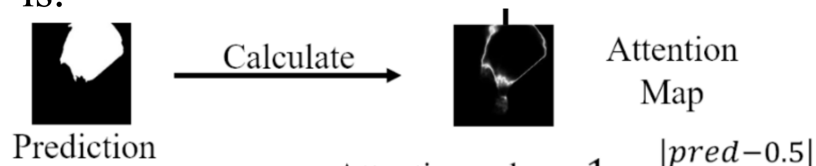

$$\text{Attention value} = 1 - \frac{|pred - 0.5|}{0.5}$$

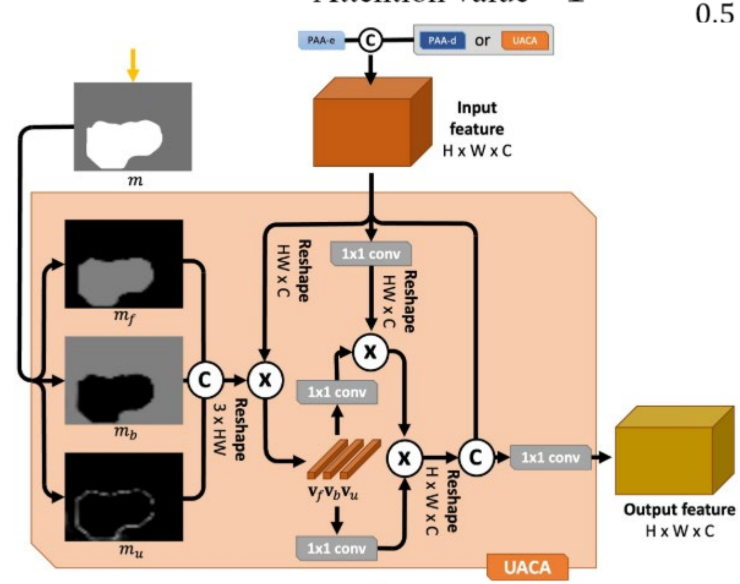

- Zhang R, et al. Adaptive context selection for polyp segmentation, MICCAI 2020.
- Kim T, Lee H, Kim D. Uacanet: Uncertainty augmented context attention for polyp segmentation, ACM International Conference on Multimedia. 2021: 2167-2175.

方法：Fundamentals of Fuzzy Logic

- **布尔逻辑的概念：**经典布尔逻辑指事物都可以用**二元项**（0或1，黑或白，是或否）来表达，而生活中，很多概念都无法用确定性的语言描述，**多与少，高于矮，年轻与年老**，这些都无法用具体的数值来进行衡量，具有模糊性。
- **模糊逻辑的概念：**模糊逻辑（Fuzzy Logic）是一种使用隶属度代替布尔真值的逻辑。模糊逻辑并不把一个命题直接分为真与假，而对于真与假的归属，可以用隶属度来进行衡量。**隶属度**是[0,1]之间的一个取值，用来标识一个程度。
- **布尔与模糊逻辑运算对比：**

Boolean Logic	Fuzzy Logic
AND(x,y)	MIN(x,y)
OR(x,y)	MAX(x,y)
NOT(x)	1-x

- https://blog.csdn.net/SweeNeil/article/details/86535572
- https://www.jianshu.com/p/b316acff0f02

方法：Fuzzy attention derivation block

- For a specific channel c, M **membership functions** are applied to each feature point in the channel. It should be noted that M is kept the same for each channel of the feature map and can vary between different input feature maps.

高斯隶属函数：$Z_{m,c}(X,\mu,\delta) = e^{\frac{-(X_c-\mu_{m,c})^2}{2\delta_{m,c}^2}}$

- We employ the aggregation **operator 'OR'** to construct fuzzy feature representations, which can preserve the importance of target feature representations while eliminating irrelevant features.

通过模糊逻辑或（OR）运算进行模糊特征表示：

$$Z_c(X,\mu,\delta) = \bigvee_{m=1}^{\mathrm{M}} Z_{m,c}(X,\mu,\delta) = \bigvee_{m=1}^{\mathrm{M}} e^{\frac{-(X_c-\mu_{m,c})^2}{2\delta_{m,c}^2}}$$

$$= \max\left(e^{\frac{-(x_c-\mu_{1,c})^2}{2\sigma_{1,c}^2}}, \cdots, e^{\frac{-(X_c-\mu_{m,c})^2}{2\delta_{m,c}^2}}, \cdots, e^{\frac{-(x_c-\mu_{M,c})^2}{2\delta_{M,c}^2}}\right)$$

- The fuzzy degree tensor: $F_{Fuz}^{(i)} = \{Z_c(X,\mu,\delta)\}(c = 1, \ldots, C\big)$

- The final result of the BCE module:

$$F^{(i)} = \left(F_{Unc}^{(i)} \oplus F_{Fuz}^{(i)}\right) \oplus UpSample\left(F_h^{(i+1)}\right)$$

方法: Trajectory Continuity Enhancement Module

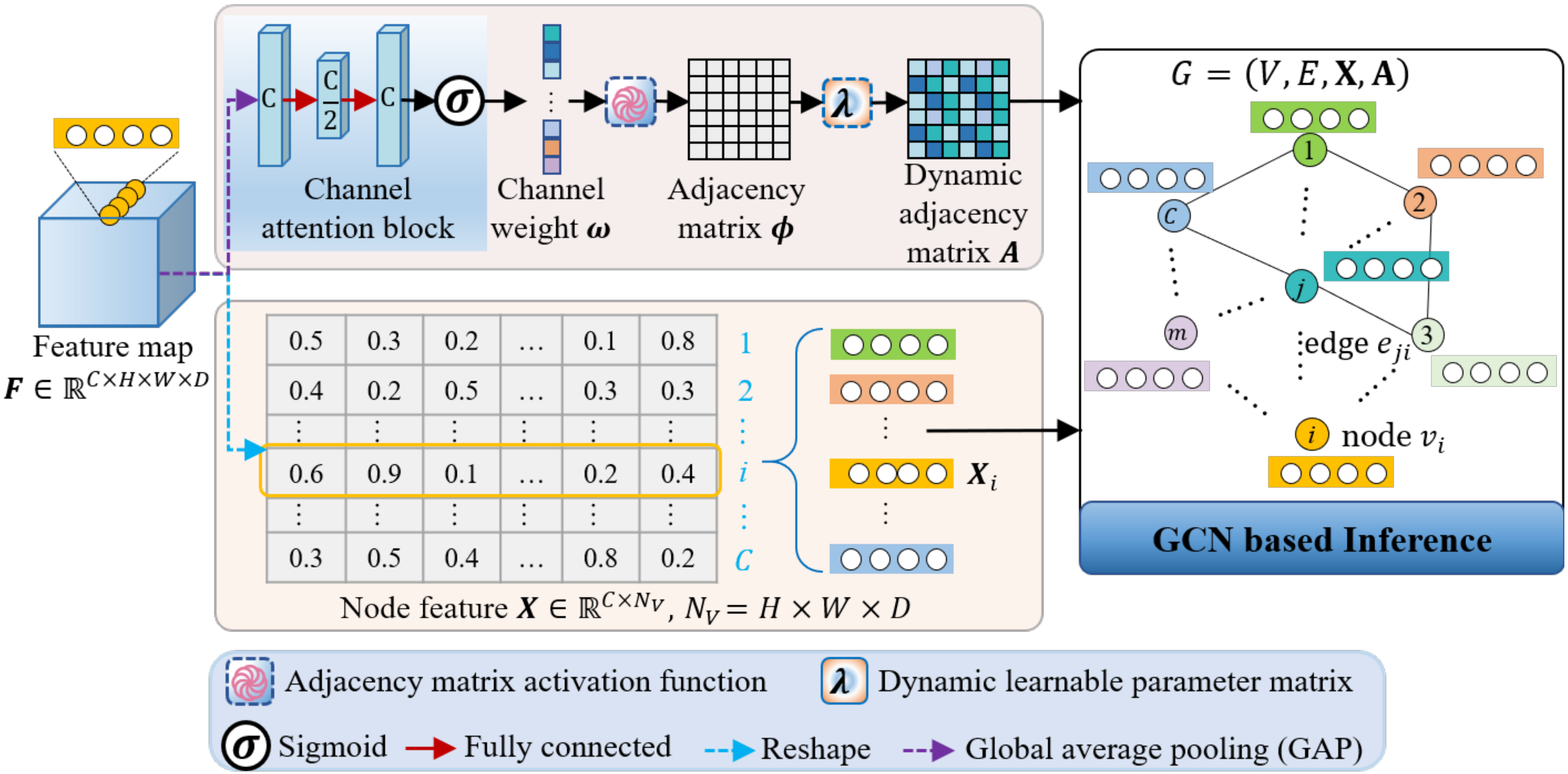

We propose a TCE module embedded at the bottom of the network, built upon a 3D dynamic GCN with adaptive hyper-parameter optimization, capable of iteratively improving vessel trajectory continuity.

实验结果：定量结果

Table 1: The mean±std results of CA segmentation performance on the CAS-119 dataset and the ASOCA dataset by different methods. The best results are in **bold**, and the second-best results are underlined.

Datasets	Method	DSC (%)↑	TPR (%)↑	ASSD (*mm*)↓	TR (%)↑	TP (%)↑	p-value (DSC)
CAS-119	UNet3D (Çiçek et al., 2016)	81.65±0.73	88.16±0.78	1.56±0.05	87.93±0.98	90.04±0.82	7.68×10^{-5}
	VNet (Milletari et al., 2016)	81.78±0.62	88.32±0.69	1.51±0.04	88.08±0.81	90.22±0.78	8.35×10^{-6}
	HighResNet3D (Li et al., 2017)	82.57±0.84	88.49±0.73	1.31±0.06	88.15±0.58	90.95±0.66	1.73×10^{-5}
	MedT (Valanarasu et al., 2021)	82.22±0.77	88.72±0.63	1.58±0.07	89.74±0.61	90.62±0.74	7.66×10^{-4}
	TransBTS (Wang et al., 2021)	82.53±0.72	88.79±0.55	1.52±0.05	89.12±0.72	90.94±0.83	8.92×10^{-4}
	Unetr (Hatamizadeh et al., 2022)	83.01±0.57	89.14±0.53	1.41±0.06	89.77±0.85	91.07±0.79	1.36×10^{-5}
	CA-Net (Gu et al., 2020)	83.67±0.84	89.87±0.55	1.42±0.06	89.93±0.69	91.84±0.88	7.69×10^{-4}
	MTLN (Zhang et al., 2021)	83.72±0.78	89.93±0.81	1.19±0.05	89.76±0.78	91.93±0.94	9.55×10^{-5}
	CPFNet (Feng et al., 2020)	84.01±0.68	90.31±0.45	1.08±0.06	90.36±0.82	92.87±0.86	1.37×10^{-4}
	DenseVoxelNet (Yu et al., 2017)	83.35±0.58	88.72±0.67	1.13±0.05	89.85±1.02	91.64±0.85	7.43×10^{-4}
	CS^{2}Net (Mou et al., 2021)	84.34±0.46	90.76±0.84	1.02±0.05	90.25±0.83	92.95±0.89	1.85×10^{-4}
	MsCAS (Dong et al., 2022)	84.58±0.45	89.39±0.34	0.83±0.04	90.05±0.74	92.74±0.92	8.92×10^{-4}
	BT-Net	**86.27±0.31**	**92.31±0.27**	**0.79±0.04**	**92.37±0.59**	**95.16±0.75**	–
ASOCA	UNet3D (Çiçek et al., 2016)	83.84±0.81	88.51±0.83	1.21±0.12	87.84±0.85	90.36±0.77	6.47×10^{-6}
	VNet (Milletari et al., 2016)	83.96±0.94	88.73±0.65	1.26±0.10	88.36±0.76	90.57±0.72	2.13×10^{-5}
	HighResNet3D (Li et al., 2017)	84.25±0.87	89.26±0.68	1.19±0.08	88.72±0.49	91.25±0.67	6.52×10^{-4}
	MedT (Valanarasu et al., 2021)	84.43±0.82	89.34±0.81	1.27±0.10	88.65±0.65	90.91±0.59	7.82×10^{-5}
	TransBTS (Wang et al., 2021)	84.76±1.04	89.68±0.84	1.23±0.11	89.06±0.73	91.21±0.67	8.77×10^{-5}
	Unetr (Hatamizadeh et al., 2022)	85.22±0.91	88.11±0.77	1.16±0.07	89.49±0.56	92.35±0.54	1.65×10^{-4}
	CA-Net (Gu et al., 2020)	85.85±0.86	90.64±0.63	1.61±0.08	90.89±0.82	92.78±0.79	9.52×10^{-4}
	MTLN (Zhang et al., 2021)	85.91±0.79	91.05±0.67	1.05±0.11	90.82±0.92	92.89±1.01	5.37×10^{-4}
	CPFNet (Feng et al., 2020)	86.23±0.72	91.24±0.52	0.86±0.09	91.37±0.76	93.52±0.78	4.57×10^{-4}
	DenseVoxelNet (Yu et al., 2017)	85.54±0.88	90.21±0.69	0.85±0.10	90.91±0.96	92.72±1.16	9.36×10^{-5}
	CS^{2}Net (Mou et al., 2021)	86.67±0.91	91.01±0.72	0.81±0.07	91.32±0.79	93.56±0.78	3.28×10^{-4}
	MsCAS (Dong et al., 2022)	86.53±0.68	90.85±0.46	0.78±0.09	91.11±0.68	93.44±0.86	5.81×10^{-4}
	BT-Net	**88.78±0.44**	**92.86±0.43**	**0.57±0.08**	**92.46±0.63**	**94.67±0.56**	–

实验结果：定性结果CAS-119 数据集

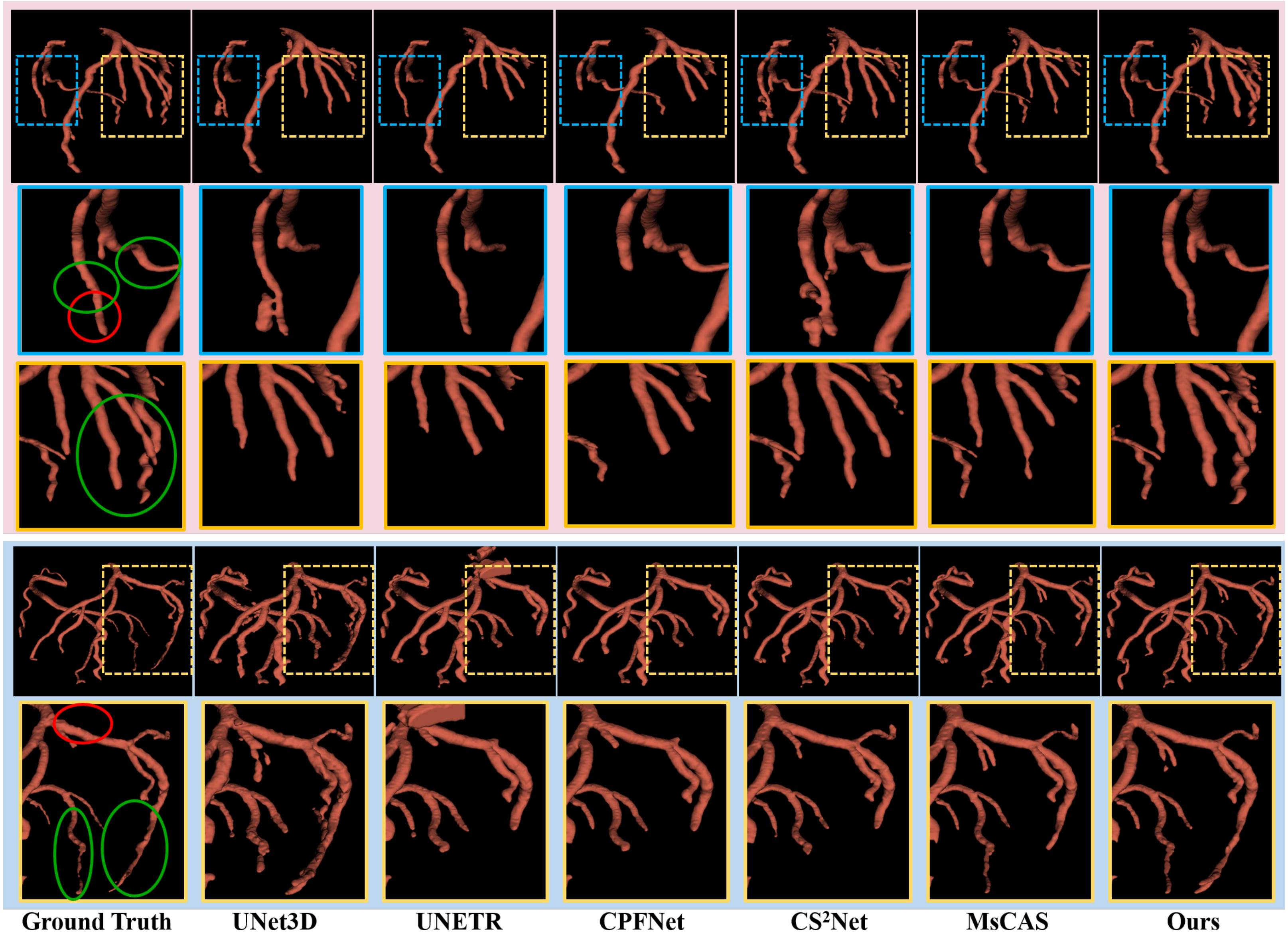

实验结果：定性结果ASOCA 数据集

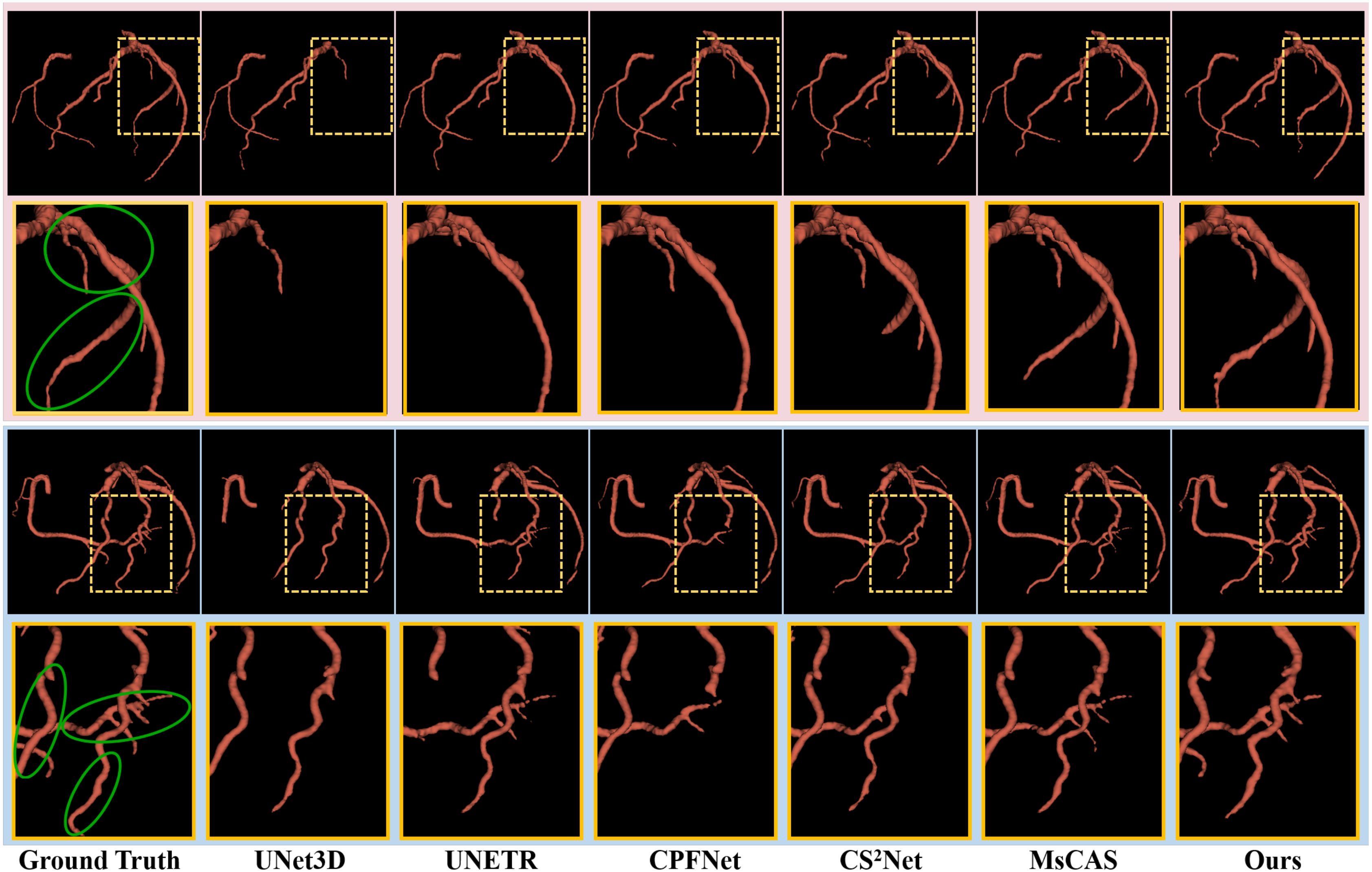

实验结果：其他血管数据集

Table 2: Quantitative comparison of our method with other methods on the PVS-203 and MIDAS datasets. The best results are in bold.

Datasets	Method	DSC (%)↑	TPR (%)↑	ASSD (*mm*)↓	TR (%)↑	TP (%)↑	p-value (DSC)
PVS-203	UNet3D (Çiçek et al., 2016)	87.02±0.46	85.76±0.56	1.42±0.11	87.09±0.53	87.94±0.67	6.48×10^{-5}
	VNet (Milletari et al., 2016)	87.51±0.47	86.22±0.52	1.38±0.09	87.60±0.55	88.12±0.64	5.59×10^{-5}
	CPFNet (Feng et al., 2020)	89.24±0.42	88.57±0.49	1.29±0.10	91.34±0.61	90.85±0.62	3.27×10^{-4}
	CS^{2}Net(Mou et al., 2021)	90.01±0.38	90.15±0.47	1.21±0.09	91.27±0.55	91.88±0.56	8.76×10^{-3}
	BT-Net	**91.44±0.35**	**92.78±0.44**	**1.16±0.08**	**93.12±0.52**	**94.61±0.57**	–
MIDAS	UNet3D (Çiçek et al., 2016)	66.72±0.73	73.38±0.64	1.53±0.10	78.44±0.83	81.64±0.82	1.54×10^{-3}
	VNet (Milletari et al., 2016)	67.01±0.68	73.22±0.67	1.49±0.12	78.57±0.76	81.86±0.76	8.81×10^{-4}
	CPFNet (Feng et al., 2020)	68.56±0.71	74.61±0.59	1.30±0.09	80.12±0.78	83.13±0.79	5.32×10^{-3}
	CS^{2}Net(Mou et al., 2021)	69.33±0.69	75.41±0.52	1.22±0.12	80.60±0.75	83.77±0.81	0.027
	BT-Net	**71.82±0.65**	**76.39±0.48**	**1.14±0.10**	**82.12±0.64**	**85.92±0.78**	–

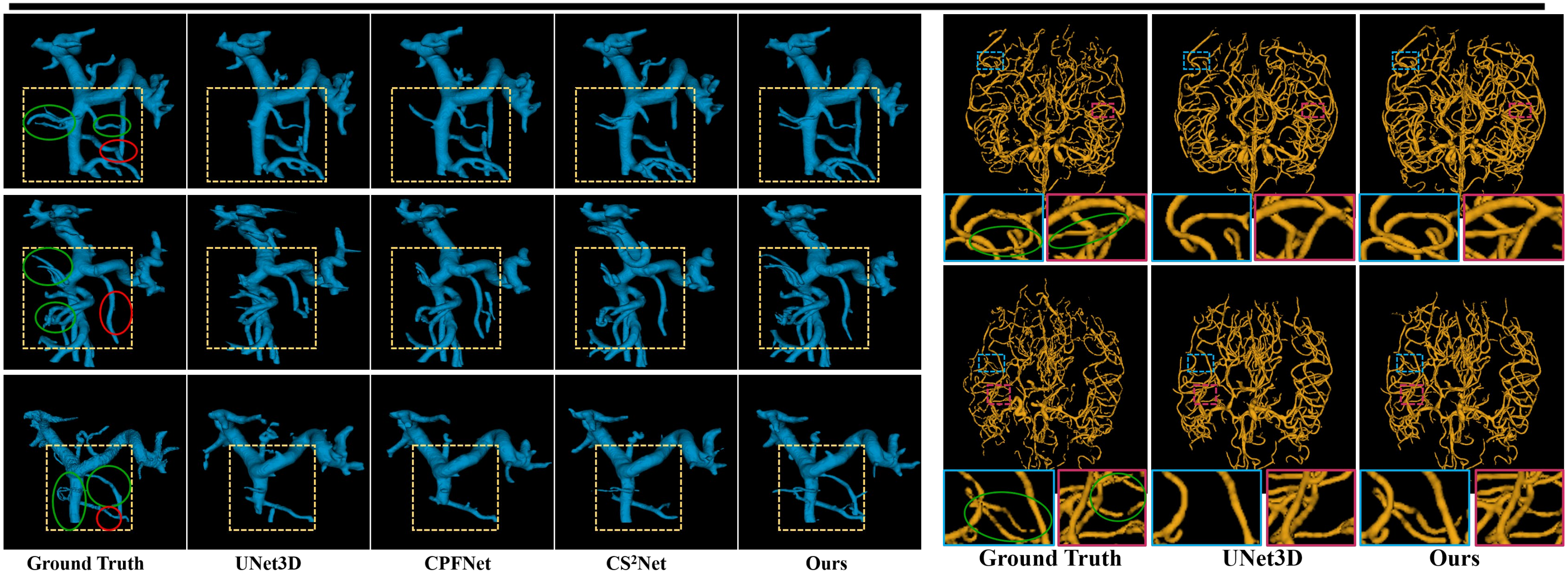

谢 谢！